Desalination and Water Treatment
www.deswater.com

doi: 10.1080/19443994.2016.1159251

57 (2016) 26073–26088
November

Taylor & Francis
Taylor & Francis Group

Effect of surfactant and sonication on Pd(II) adsorption from synthetic electroless plating solutions using commercial activated charcoal adsorbent

Yennam Rajesh, Uppaluri Ramagopal*

Department of Chemical Engineering, Indian Institute of Technology Guwahati, Guwahati 781039, Assam, India, Tel. +91 361 2582260; Fax: +91 361 2582291; emails: rajeshiitg09@gmail.com (Y. Rajesh), ramgopalu@iitg.ernet.in (U. Ramagopal)

Received 7 August 2015; Accepted 21 February 2016

ABSTRACT

This work addresses the evaluation of Pd(II) adsorption characteristics on commercial activated charcoal using synthetic electroless plating solutions with and without cationic surfactant. The experimental investigations involved wider Pd (50–500 mg/L) and surfactant solution concentrations (1–4 CMC). Surface characterization was conducted using Brunauer–Emmett–Teller analysis, Fourier transform infrared spectroscopy, laser particle size analysis, scanning electron microscopy and energy dispersive X-ray spectroscopy techniques. It was observed that the Pd(II) adsorption characteristics from synthetic electroless plating solutions were distinct and referred to lower metal uptake and removal efficiency. The presence of CTAB surfactant significantly altered the adsorption characteristics with higher surfactant concentrations providing higher metal uptake and removal efficiency. Both agitation- and sonication-assisted adsorption were deployed to identify the optimal process parameters. The optimal batch adsorption process parameters have been evaluated to be 300 min, 10, 6 g/L, 500 mg/L and 4 CMC for contact time, pH, adsorbent dosage, Pd solution concentration and surfactant solution concentration, respectively. For these conditions, the maximum metal uptake and removal efficiency have been evaluated to be 62.46 mg/g and 93.82%, respectively. Further, it was evaluated that the sorption data fit well with Freundlich isotherm model and pseudo-second-order kinetic model. Also, the evaluated thermodynamic model parameters confirm endothermic nature of adsorption.

Keywords: Commercial activated carbon; Palladium; Surfactant; Sonication; Electroless plating solution; Adsorption

1. Introduction

With stringent environmental legislations and increasing costs of noble metals, there is a growing emphasis towards the recovery and reuse of noble metals from waste solutions. As per OSHA, the permissible exposure limit for Pd is about 5 mg/L [1]. From a hazard perspective, Pd solutions cause skin sensitization, eye or respiratory tract irritation and are carcinogenic in nature. Above Pd solution concentrations of 3 mg/L, they may even cause bone marrow, liver and kidney damages [2]. Palladium recovery is especially desired from spent nuclear fuel waste [3], electroplating [4] and electroless plating solutions [5]. Several technologies such as solid phase extraction, solvent extraction, electrochemical recovery, precipitation and membrane separation were proposed and

---

*Corresponding author.

investigated for the recovery of platinum group metals [4–6]. Palladium recovery from spent waste solutions using adsorption technology enables the generation of noble metal rich adsorbent which can be used as a catalyst in chemical and environmental engineering applications.

Till date, simple and inexpensive adsorbents such as activated carbons and modified activated charcoal with polymer [6], carbon pellets [7], cross-linked chitosan resin [8], tannin gel [9], racomitriumlanuginosum [10], bayberry tannin immobilized collagen fibre (BTICF) [11], carbonaceous adsorbents [12], aminated lignin derivatives [13], anion exchange resins and activated carbon [14], thiourea-modified chitosan microspheres [15] have been studied for the Pd(II) adsorption from synthetic palladium aqueous solutions. For several cases corresponding to waste stream complexity, complex adsorbent resin such as Amberlite [16] has been evaluated. Among these adsorbents, activated charcoal appears to be highly efficient for the recovery of palladium from waste streams with relatively less complexity in terms of the chemical constituents in the stream. Activated charcoal possesses high adsorption capacity, adsorption rate, good resistance to abrasion, etc., and was proven for its utility towards adsorption of gases, reactive dyes, heavy metals and precious metals such as platinum, palladium, gold and silver.

A detailed study of available literature affirmed that commercial activated charcoal possessed an adsorption capacity of 35.7 and 45.5 mg/g for Pd and Pt, respectively, from an aqueous solution with 300 mg/L concentration [6]. Corresponding removal efficiency for both the metals was reported to be 98%. The equilibrium adsorption data were well described by the Langmuir and Freundlich models and the adsorption kinetics of Pd and Pt followed pseudo-second-order model [6].

A critical observation of the available literature indicates that very few literatures addressed the dependence of adsorption characteristics on solution complexity. While data with respect to platinum group metals are scarce, few literatures are available with respect to the adsorption of heavy metals. These literatures do not outline a systematic investigation with respect to the effect of surfactant and solution complexity on adsorption. On the other hand, the role of ultrasound as a mass transfer enhancement technique to supplement the adsorption of precious metals has not received any attention till date.

Hence, the combinatorial role of stabilizer, liquor ammonia and surfactants to influence the adsorption characteristics of palladium over activated charcoal has not received any attention and is the objective of the present work. Another objective of this work is to evaluate the potential of ultrasound-assisted adsorption for Pd recovery from electroless plating solutions.

This work addresses the adsorption characteristics of palladium from simulated electroless plating solutions using commercial activated carbon. Adsorption characterization has been carried out using Fourier transform infrared spectroscopy (FTIR), Brunauer–Emmett–Teller analysis (BET), laser particle size analysis (LPSA), scanning electron microscopy (SEM) and energy dispersive X-ray spectral analysis. The role of sonication as a supplement to favour mass transfer enhancement has also been investigated for various cases. For optimized adsorbent dosage, contact time and pH, adsorption experiments were conducted for wider Pd(II) solution concentrations (50–500 mg/L). The specific influence of various additives such as CTAB (surfactant), Na_2EDTA (stabilizer) and liquor ammonia (NH_3) on the adsorption of Pd(II) using commercial activated charcoal has been addressed. Equilibrium adsorption data have been tested using various isotherm models such as Langmuir and Freundich models. The adsorption kinetics were evaluated using both pseudo-first-order and second-order kinetic models. The next section summarizes adsorption and characterization details.

2. Materials and methods

2.1. Materials

Commercial activated charcoal (AC) (CAS No. 7440-44-0) was purchased from Merck India Limited, Mumbai and was used as the adsorbent. $PdCl_2$ (99.9% pure obtained from SRL Chemicals Pvt. Ltd, India), Na_2EDTA (Merck India), NH_4OH (25%) (Merck India), N-Cetyl-N,N,N-Trimethyl Ammonium Bromide (CTAB) (Merck India Ltd), and Millipore water (Make: milliQ) were used for the preparation of metal solutions.

2.2. Preparation of the adsorbate using Pd electroless plating solution

The stock solution of Palladium chloride (500 ppm) was prepared using a composition similar to the spent electroless plating bath composition (Table 1). Precisely, it refers to the inclusion of a stabilizer (Na_2EDTA) and an optional cationic surfactant (CTAB) in a highly alkaline solution along with liquor ammonia. The Pd concentration of the prepared solutions for adsorption experiments were varied from 50 to 500 mg/L using dilution principle. For all adsorption

Table 1
Compositions of synthetic electroless plating solutions

Name of the component	Palladium solution concentration (mg/L)					
	50	100	200	300	400	500
$PdCl_2$ (mg/L)	83.31	166.63	333.27	499.90	666.54	833.17
Na_2EDTA (g/L)	1.39	1.39	1.39	1.39	1.39	1.39
NH_3 solution (25%), mL/L	10.33	10.33	10.33	10.33	10.33	10.33
CTAB, mg/L (if any)	335–1,340	335–1,340	335–1,340	335–1,340	335–1,340	335–1,340

experiments, the pH of the diluted solutions was adjusted using analytical grade HCl and NaOH solutions.

2.3. Characterization of adsorbents

FTIR (Perkin–Elmer Spectrum one), SEM (Oxford, Leo 1430VP), energy dispersive spectral (Oxford, Leo 1430VP), Brunauer–Emmett–Teller (BET) surface area analyser (Beckman-Coulter, SA 3100), LPSA and zero point charge (PZC) (Malvern Instruments Ltd) techniques were used for adsorbent characterization. Procedures for these techniques are similar to those presented in our earlier work [17].

2.4. Batch adsorption experiments

Batch mode experiments were carried out using 1 g of activated charcoal powder with 50 mL of synthetic electroless plating solution. The experiments were performed in a wrist action shaker (make: Lab Tech., India) for initial concentrations of 50–500 mg/L and a time period of 360 min at 200 rpm in 250-mL flasks containing 50 mL of solutions at room temperature (25˚C). Continuous mixing was facilitated during the experimental period at a constant agitation speed of 200 rpm so as to ensure the attainment of mass transfer equilibrium. Subsequently, the mixture was filtered using Whatman filter paper (No. 40) to obtain the spent electroless plating solution whose Pd(II) concentration was determined at a wavelength of 247.8 nm using atomic absorption spectrophotometer (AAS) (Make: Varian spectra, FS240) equipped with air-acetylene burner. The AAS instrumental parameters refer to the operation of the instrument in air acetylene mode, slit width of 1.0 nm, lamp current of 4 mA, measurement time of 1.5 s, air flow of 3.5 L/min and acetylene flow of 1.5 L/min [18]. Based on the calibration chart prepared prior using precise concentrations of synthetic ELP solutions, the Pd(II) solution concentrations in the feed and effluent samples were evaluated. Using the measured concentrations, adsorption parameters namely q_{eq} (amount of adsorption at equilibrium) and metal removal % were estimated using the following equations:

$$q_{eq} = \frac{(C_o - C_{eq})V}{W} \tag{1}$$

$$\text{Removal }\% = \frac{(C_o - C_{eq})}{C_o} \times 100 \tag{2}$$

where C_o is the initial concentration of Pd(II) in aqueous solution (mg/L), C_{eq} is the equilibrium adsorption concentration of Pd(II) (mg/L), V is the volume of aqueous solution (ml), W is the weight of the adsorbent dosage (g) and q_{eq} is the adsorption capacity t at equilibrium (mg/g).

For the experiments conducted with CTAB surfactant-containing solutions, the solution concentration of CTAB surfactant was varied in the range of 1—4 CMC (335–1,340 mg/L). Further, few batch adsorption experiments were conducted by deploying sonication-assisted adsorption instead of physisorption. These experiments involved placing the adsorbent and adsorbate solution in an ultrasonic cleaning bath (Make: Elma S30 H) at a temperature of 30˚C under degas mode for a time period of 120 min to facilitate equilibrium. For all cases, obtained data have been compared with the data provided by Sharififard et al. [6], given the fact that most other literatures do not refer to activated carbon adsorbent material. Further, literature comparison with the data available from other competent literature [7] has not be considered given the inferiority of data trends reported in the literature in comparison with those presented by Sharififard et al. [6].

2.5. Adsorption equilibrium models

The fitness of measured equilibrium adsorption data to standard equilibrium models was evaluated for Langmuir and Freundlich isotherms, which are typically expressed as [19–21]:

$$\frac{C_{\mathrm{eq}}}{q_{\mathrm{eq}}} = \frac{1}{bq_{\max}} + \frac{1}{q_{\max}} C_{\mathrm{eq}} \tag{3}$$

$$\log q_{\mathrm{eq}} = \log K_{\mathrm{F}} + n \log C_{\mathrm{eq}} \tag{4}$$

where $q_{\max}$ is the Langmuir monolayer adsorption capacity (mg/g), b is the Langmuir equilibrium constant, n is the Freundlich constant, and K_{F} is the Freundlich isotherm coefficient.

Pseudo-first-order, pseudo-second-order and intraparticle diffusion models were tested for their fitness to represent the kinetics of Pd(II) adsorption on activated charcoal adsorbent. These were presented as follows [22–25]:

$$\log(q_{\mathrm{eq}} - q_t) = \log(q_{\mathrm{eq}}) - \frac{k_1}{2.303} t \tag{5}$$

$$\frac{t}{q} = \frac{1}{k_2 q_{\mathrm{eq}}^2} + \frac{1}{q_{\mathrm{eq}}} t \tag{6}$$

$$q_t = K_{\mathrm{id}} t^{0.5} + C \tag{7}$$

where t is the agitation time (min), k_1 is the first-order rate constant (min^{-1}), k_2 is the pseudo-second-order rate constant (g/mg/min), and K_{id} is the intra-particle rate constant (time^{-1}).

For both equilibrium and kinetic models, errors associated to the fitness of experimental data with the models were evaluated using procedures mentioned in our earlier work [17]. Thermodynamic parameters such as ΔH° and ΔS° were determined using procedures similar to those presented in our earlier work [17].

3. Results and discussions

3.1. Characterization of the adsorbent

3.1.1. Surface area analysis and particle size distribution

Adsorbents with higher BET surface area enable a reduction in adsorbent dosage and thereby enhance adsorption efficiency and reduce operating cost [26]. The surface area and pore size of the AC adsorbent was evaluated using the N_2 adsorption–desorption isotherm generated with the BET surface area analyser at 77 K. Prior to the measurement, the samples were degassed at 200˚C in vacuum for 60 min. Fig. 1(a) presents the N_2 adsorption–desorption isotherms of AC adsorbent. It can be observed that the isotherms were of type IV and H_4 hysteresis loop, which according to International Union of Pure and Applied Chemistry classification indicated the existence of narrow slit-like pores. Also, it can be seen that the isotherm grew sharply during the early stages of adsorption which is due to the micro pore filling effect. Based on the BET surface area analysis, the BET surface area, BET monolayer volume, Langmuir surface area, Langmuir monolayer volume, total pore volume value of the commercial AC adsorbent have been evaluated as 1,057.17 m^2/g, 242.89 cc/g, 1,197.5 m^2/g, 275.123 cc/g and 0.9814 ml/g, respectively.

Fig. 1(b) represents adsorption- and desorption-based Barrett–Joyner–Halenda (BJH) pore size distribution [26–28] of AC. The pore size distribution indicated that the adsorbent possessed cylindrical pores and the BJH analysis provided sharper peaks than the isotherm data presented in Fig. 1(a). Fig. 1(c) illustrates the variation in pore area distribution with pore diameter. It can be seen that the pore area of the adsorbent was more sensitive with respect to the adsorption but not desorption process which is in agreement with the trends presented in the literature [26–28]. In summary, the surface area analysis indicated that the AC possessed good surface texture and pore size distribution.

Fig. 1(d) represents the particle size distribution of activated charcoal, using which the average particle size of the AC was evaluated as 25.47 μm. The narrow particle size distribution and lower average particle size of the adsorbent is promising, given the fact that particle size strongly influences the metal uptake and efficiency [6,27].

3.1.2. FTIR analysis

FTIR analysis was conducted for both raw AC sample and AC samples obtained after Pd(II) batch adsorption experiments. The FTIR analysis (Fig. 2) indicated the existence of several functional groups on the adsorbent surface. For the raw sample (AC), several peaks were found at the wave number values of 3,722, 3,616, 3,296, 2,333, 1,700, 1,521, 1,340 and 956 cm^{-1}. For the case where adsorbent was contacted with Pd aqueous solutions, peaks were observed at wave numbers of 3,736, 3,624, 3,288, 2,970, 2,416, 2,301, 1,706, 1,510, 1,338 and 962 cm^{-1}. For the AC adsorbent that was contacted with Pd, Na_2EDTA and liquor NH_3 but not CTAB, the peaks were observed at wave numbers of 2,924.1, 2,858.9, 2,364.7 and 2,330.3 cm^{-1}. On the other hand, for the case of AC that was contacted with CTAB using both agitation and sonication-assisted adsorption, the peaks were observed at 3,738, 3,612, 3,288, 2,970, 2,414, 2,291,

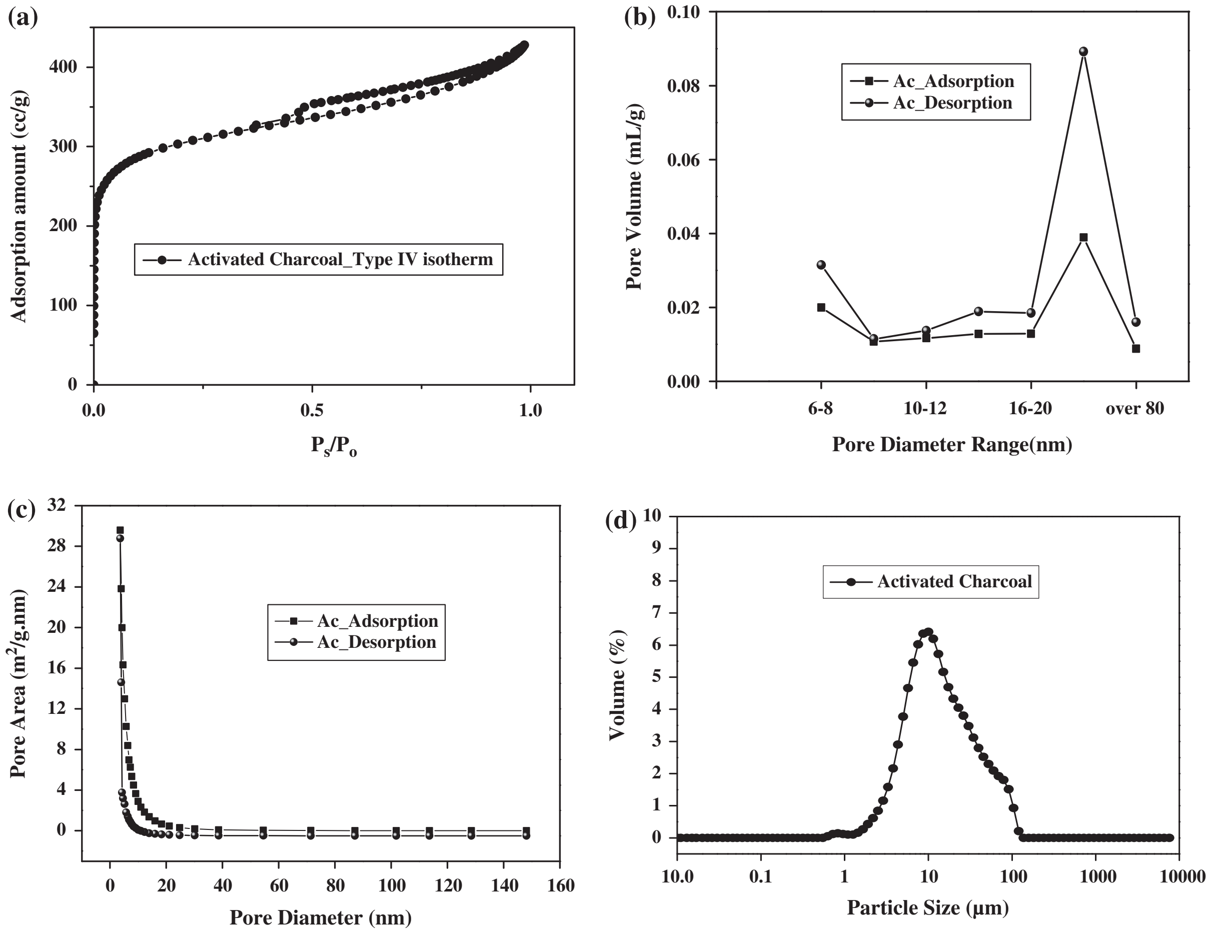

Fig. 1. Surface properties of commercial AC adsorbent (a) hysteresis isotherm (BET), (b) variation of pore volume with pore diameter (BET), (c) variation of pore area with pore diameter (BET) and (d) particle size distributions (LPSA).

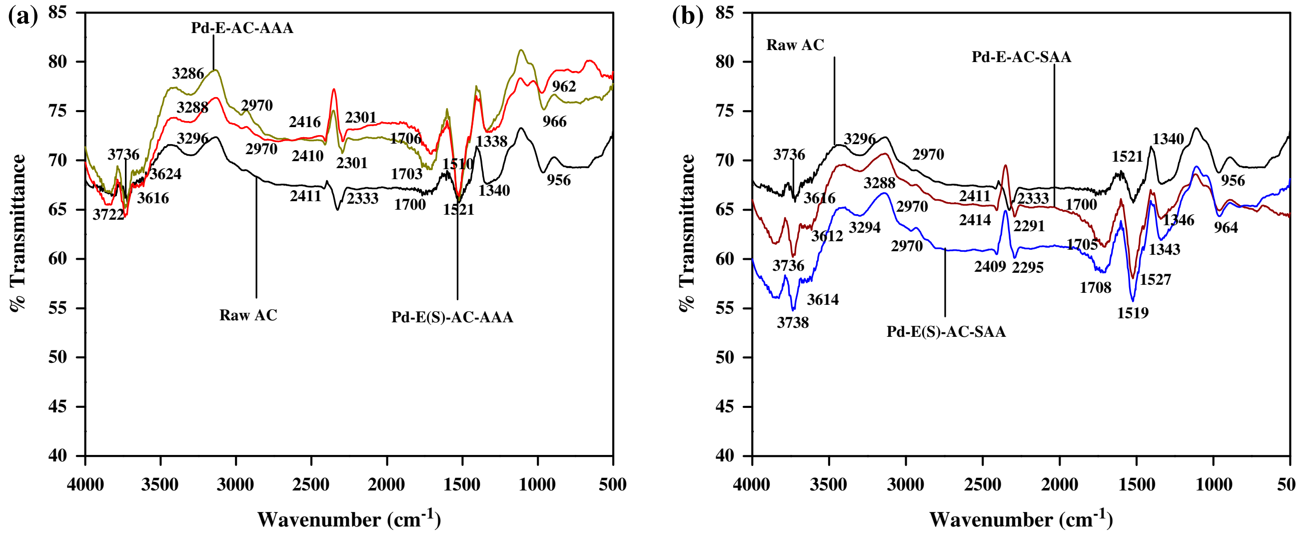

Fig. 2. FTIR spectra of AC adsorbent before and after Pd adsorption for (a) agitation and (b) sonication-assisted Pd(II) adsorption.

1,705, 1,527, 1,346 and 964 cm^{-1} with a distinct peak observed at 966 cm^{-1} for the case of agitation-assisted adsorption. Therefore, comparing the FTIR peaks obtained for all cases, Pd(II) adsorption corresponds to common peaks that were obtained at wave numbers of 3,736, 3,624, 3,288, 2,970, 2,416, 2,301, 1,706, 1,510, 1,338 and 962 cm^{-1} and Pd(II) adsorption in the presence of CTAB indicated the existence of two additional peaks at 1,706 and 962 cm^{-1}. Also, several spectral peaks can be observed to have shifted from low to high intensity. Among various observed spectral peak shifts, some functional group interactions affirm C–H aliphatic stretching (2,920.2 cm^{-1}), –O–CH_3 of aldehyde group (2,858.5 cm^{-1}), stretching of C–O or O–H deformation in carboxylic acids (1,647.3 cm^{-1}). Thus, it is apparent that Pd(II) interaction with carbonyl and carboxyl groups enabled shift in the peaks and their intensities and thereby infer that palladium ions have chemical interaction with surface chemical groups of activated charcoal during the adsorption process. The chemical interactions and bond formations of Pd(II) with carbonyl and carboxylic groups are due to the lone pair of electrons present on O atom and due to the partial negative charge present on both C and O atoms, which is dependent on the direction in which the bond shift occurs [6,29,30].

3.1.3. SEM analysis

Fig. 3(a)—(i) and (ii) respectively illustrate the SEM-based surface morphology of the raw adsorbent (AC) and adsorbent subjected to adsorption with synthetic Pd(II) electroless plating solution. It can be observed from the SEM images that palladium adsorption is occurred during adsorption and this is confirmed as a new bulky coated layer on the porous surface. In other words, Pd occupied the porous surface texture of the AC. Similar inferences have been presented by Sharififard et al. [6].

3.1.4. Energy dispersive X-ray spectroscopy analysis

Fig. 3(b)—(i) and (ii) present the EDX spectra of the raw adsorbent and Pd adsorbed AC, respectively. It was observed in the spectra that for the raw adsorbent case, carbon and oxygen elements existed on the adsorbent surface. This is in accordance with the literature data presented by Sharififard et al. [6], where it was conveyed that raw AC adsorbents constitute several carbon and oxygen groups that could be acidic (carboxylic and lactonic), non-acidic (ether, quinine and carbonyl), phenolic and anhydride functional groups. Further, for the Pd-adsorbed AC, it can be observed that in addition to the carbon and oxygen peaks, Pd-specific peaks have been identified in the energy dispersive X-ray spectroscopy (EDS) analysis. For the commercial AC adsorbent, the EDS-based analysis indicated 88.7 and 11.23 wt% for carbon and oxygen, respectively, on the adsorbent surface. After adsorption with 500 mg/L initial Pd solution concentration, carbon oxygen and palladium content in the adsorbent have been evaluated to be 52.39, 13.68 and 33.93 wt%, respectively, on the adsorbent surface. For a Pd solution concentration of 50 mg/L, corresponding Pd metal uptake on the AC adsorbent from batch adsorption experiments is 44.03 mg/g. Thus, the evaluated metal uptake and the measured Pd concentration on the adsorbent are in good agreement and this affirms that Pd is well adsorbed to the activated carbon.

3.1.5. PZC analysis

Using pH drift method, the PZC value of AC was evaluated to be 9.5. The literature value of the PZC for the AC that was kept in contact with Pd aqueous solution is about 6.5 [6]. Since the synthetic electroless plating solutions contain liquor NH_3, it is apparent that the PZC value obtained in this case is significantly high when compared to the literature value of 6.5. In conjunction with the observed Pd adsorption data which indicated higher adsorption at higher pH (above the pH of 10), the obtained PZC value of 9.5 is in accordance with the PZC hypothesis, which indicates that adsorption is always favoured when the pH is greater than the PZC. Further, the existence of optimal pH for adsorption slightly below the PZC value is also in accordance with the data reported by Sharififard et al. [6].

3.2. Batch adsorption studies

3.2.1. Optimality of adsorption process parameters

Agitation-assisted adsorption batch experiments were conducted using synthetic Pd electroless plating solutions. The composition of the solution corresponds to the data presented in Table 1 without CTAB. Based on the adsorption process variables (metal uptake and removal efficiency), preliminary batch experiments were conducted to identify optimal operating conditions such as equilibrium time (min), pH and dosage (g).

Firstly, the optimality of the contact time was targeted by considering a fixed choice of adsorbent dosage (1 g/L), pH (9–10) and initial Pd(II) solution concentration of 50 mg/L. The second set of batch adsorption experiments were conducted for the

(a)

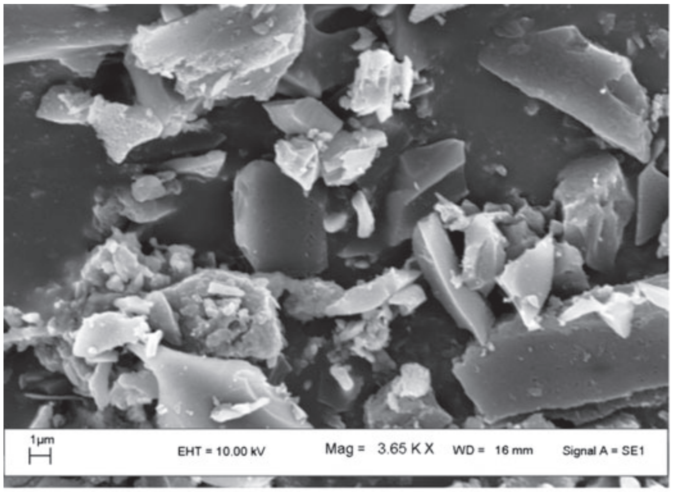

(i) Before adsorption of AC

(ii) After Pd adsorption of AC

(b)

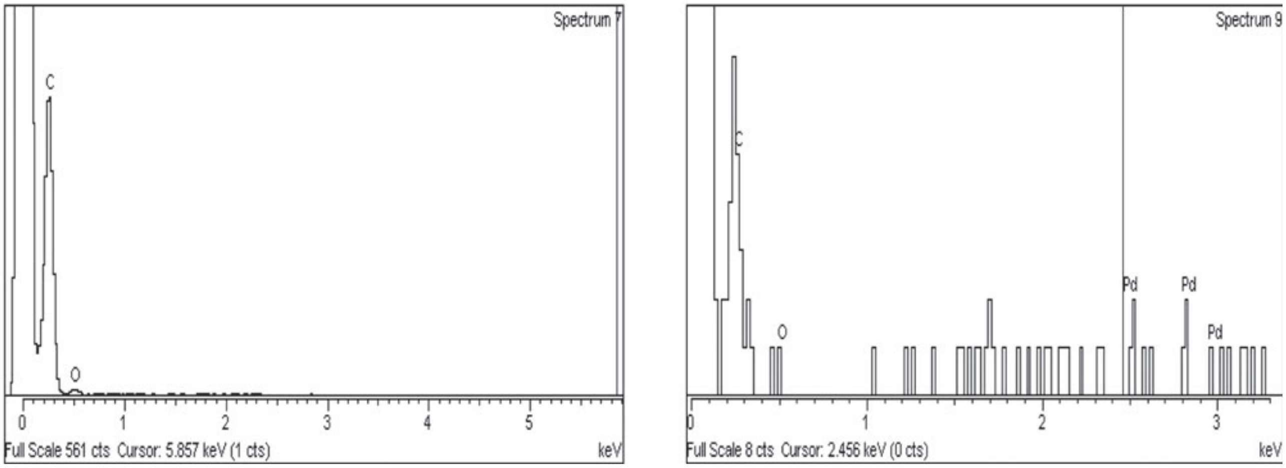

(i) Before adsorption of AC

(ii) After Pd adsorption of AC

Fig. 3. (a) Scanning electronic micrographs (SEM) of the AC adsorbent before and after agitation-assisted Pd(II) adsorption and (b) energy dispersive X-ray spectra (ED) of AC before and after Pd(II) adsorption.

corresponding optimized contact time and variant pH (2–14), fixed dosage (1 g/L) and initial Pd solution concentration of 50 mg/L. After identifying the optimal pH in the second set of batch adsorption experiments, the third set experiments were conducted for the fixed choice of contact time, pH (obtained from the second set of adsorption experiments) and Pd(II) plating solution concentration 50 mg/L, and the adsorbent dosage variation (1–6 g/L) was examined for the optimality of adsorbent variable (metal uptake and removal efficiency) profiles. Finally, the adsorption performance of AC was studied for various solution concentrations (50–500 mg/L), by selecting all the other parameters obtained from preliminary adsorption studies mentioned above. Results obtained from the three sets of adsorption experiments are presented as follows.

Fig. 4(a) shows the effect of contact time on metal uptake and removal efficiency. From the figure, it can be observed that the minimum time required to reach equilibrium (i.e. maximum adsorption) is 300 min. For this case, the maximum % removal and metal uptake (mg/g) have been evaluated as 68.4% and 34.2, respectively. Similar results were reported by Sharififard et al. [6] for Pd removal from aqueous solutions using AC adsorbent.

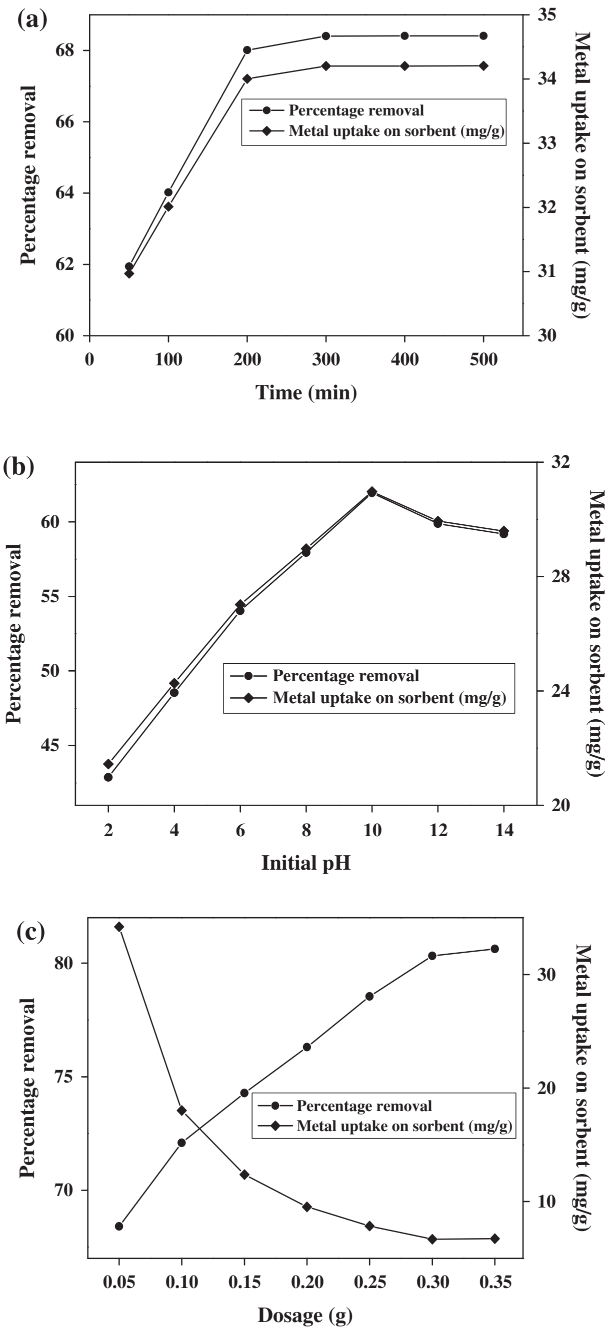

Fig. 4. Effect of adsorption parameters on the Pd(II) removal efficiency from synthetic electroless plating solutions: (a) contact time (min), (b) pH and (c) adsorbent dosage.

Fig. 4(b) presents the effect of pH on the Pd(II) adsorption characteristics using AC. It can be identified that the optimum pH was 10 where maximum % removal (62.94) and metal uptake (31.14 mg/g) have been obtained. In this regard, it is important to note that the pH of the solution affects metal ion solubility, concentrations of counter ions on the adsorbent functional groups and degree of ionization of the adsorbate. It can be observed that the metal removal increased with an increase in pH from 2 to 10 after which it steadily declined. At low pH, H^+ enables protonation effect and this does not favour the adsorption of Pd(II) on AC due to the competitive adsorption of NH_4^+ and Pd(II) on the active sites [10,11]. However, as pH increases, protonation effect reduces and the availability of OH^- on the adsorbent surface favours the electrostatic attraction of the positively charged Pd (II) ions. Beyond a pH of 10, there might be complexification of NH_3 with Pd(II), which does not favour further adsorption of Pd(II). For aqueous solutions, an optimal pH of 2 has been suggested by Sharififard et al. [6], which indicates the significance of NH_3 in affecting the optimality of pH in this work. The evaluated maximum adsorption of Pd(II) at a pH of 10 is in good agreement with the adsorption of Pd(II) from leached cyanide solutions [31,32].

The influence of adsorbent dosage on palladium removal using AC is shown in Fig. 4(c). From the figure, it can be observed that increasing adsorbent dosage from 1 to 7 g/L enhanced metal removal (80.32%), which is also in agreement with the lower average particle size (25.7 μm) of the adsorbent [6]. The enhancement of adsorption with an increase in adsorbent dosage is due to the enhancement in adsorbent surface area and availability of more metal active sites. Similar values for optimal adsorbent dosage have been presented in the literature for Pd(II) adsorption from aqueous solutions [6]. The capacity reduces with an increase in adsorbent dosage due to significant increase in the denominator (weight of adsorbent after adsorption) in comparison to the enhancement in the numerator (metal adsorbed due to more active sites).

3.2.2. *Adsorption characteristics for synthetic electroless plating solutions*

In this work, several synthetic electroless plating solution compositions have been considered to obtain insights with respect to the adsorption characteristics of Pd(II) adsorption from complex solutions. These adsorption experiments were conducted using optimized operating parameters (contact time 300 min, pH 10 and dosage 6 g/L). Various compositions investigated in this work were summarized in Table 1.

3.2.2.1. Agitation-assisted adsorption and Sonication-assisted adsorption of Pd(II) from synthetic electroless plating solutions. Fig. 5(a) presents the adsorption characteristics of Pd(II) on activated charcoal for the case involving synthetic electroless plating solutions without CTAB surfactant. As shown, for both cases, i.e. agitation-assisted adsorption (Fig. 5(a)—(i)) and sonication-assisted adsorption (Fig. 5(a)—(ii)), with on increasing Pd(II) solution concentrations, while capacity (or metal uptake) increased, the metal removal efficiency reduced. For the case of agitation-assisted adsorption, the metal uptake and removal percentage varied from 5.76–43.33 mg/g and 69.12–52%, respectively, with a variation in Pd solution concentration from 50 to 500 mg/L. On the other hand, for the sonication case, the metal uptake and removal percentage varied from 6.34–45.5 mg/g and 76.12–54.61%, respectively, with variant Pd solution concentration. Thus, it is apparent that both agitation- and sonication-assisted adsorption provided similar adsorption characteristics with only insignificant improvement in the capacity values achieved with sonication-assisted adsorption. However, it is important to note that while agitation-assisted adsorption involved a time period of 300 min, sonication-assisted adsorption was carried out for 120 min. Therefore, sonication could be considered to reduce the time required to achieve mass transfer equilibrium for Pd(II) adsorption on activated charcoal.

The enhancement in metal uptake with increasing concentration of noble metal in the solution is due to the increased driving force for mass transfer at higher concentration gradients. At lower solution concentrations,

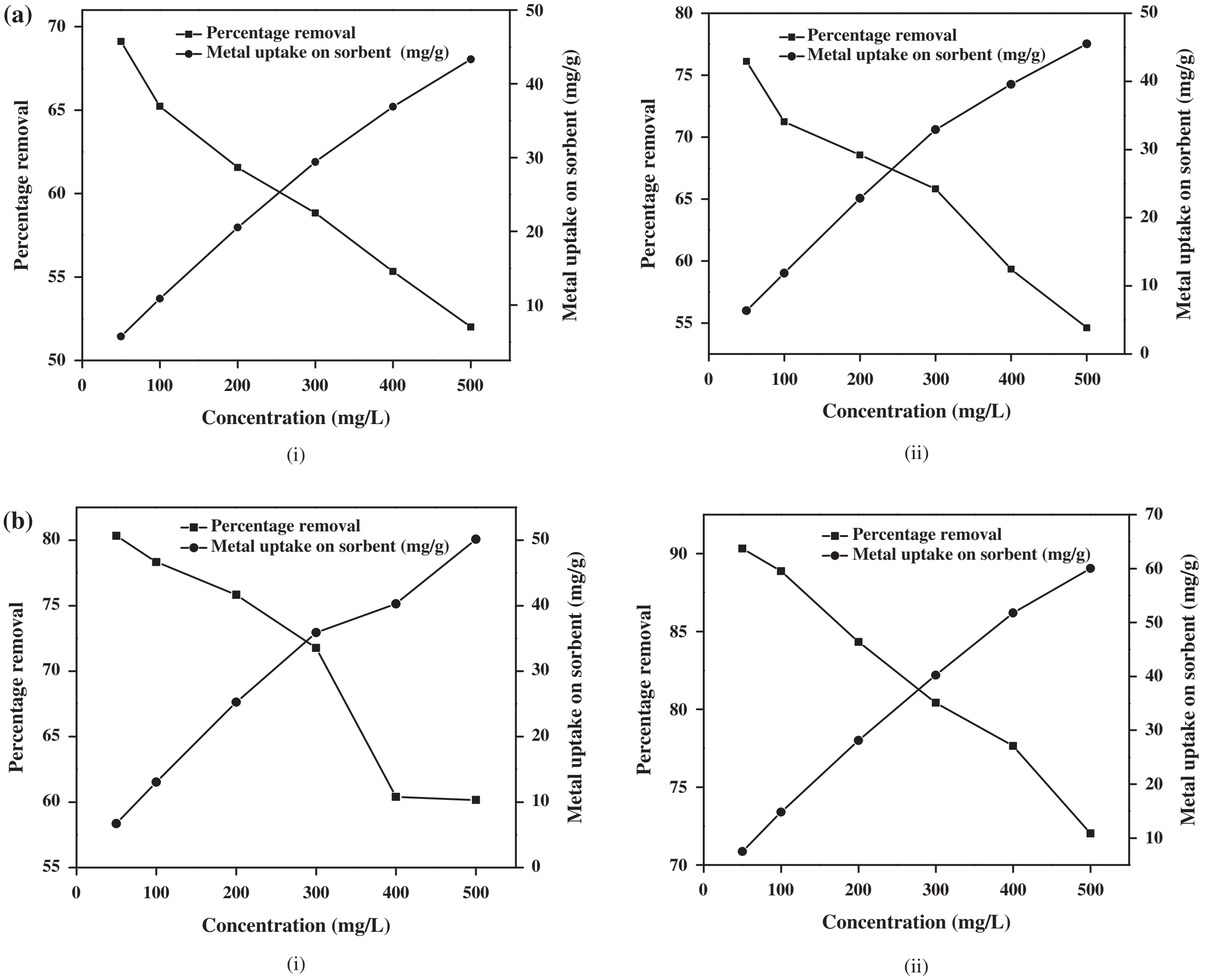

Fig. 5. (a) Pd(II) adsorption characteristics for synthetic electroless plating solutions not containing CTAB surfactant (i) agitation-assisted adsorption and (ii) sonication-assisted adsorption, (b) Pd(II) adsorption characteristics for synthetic electroless plating solutions containing CTAB (2 CMC) surfactant (i) agitation-assisted adsorption and (ii) sonication-assisted adsorption, and (c) effect of initial Pd solution concentration on the adsorption characteristics for synthetic electroless plating solutions containing CTAB surfactant (1–4 CMC)—(i) metal uptake and (ii) removal efficiency for agitation-assisted adsorption; (iii) metal uptake and (iv) removal efficiency for sonication-assisted adsorption.

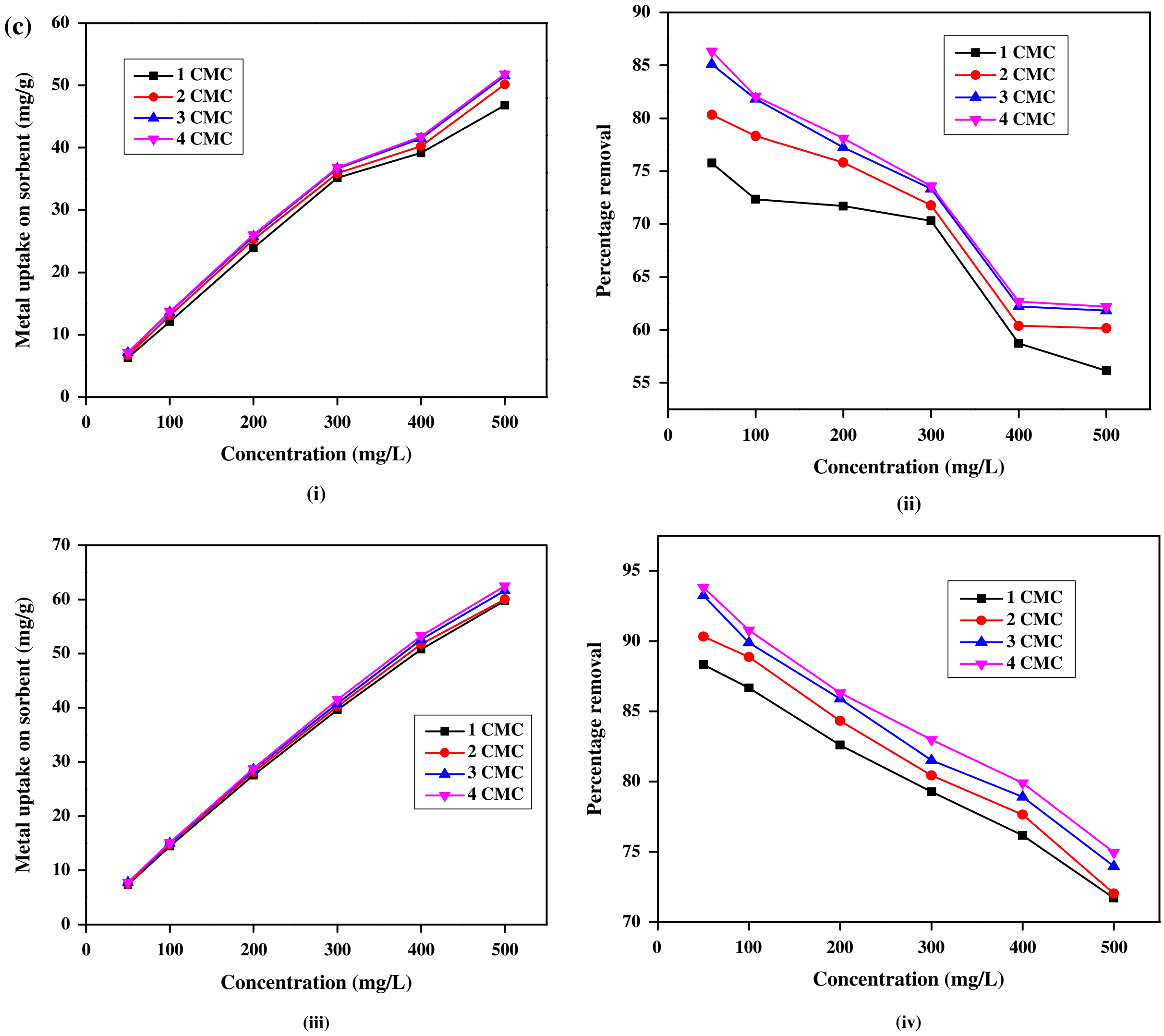

Fig. 5. (*Continued*).

Pd(II) could bind with the active sites and hence could provide higher removal efficiency. On the other hand, the reduction of metal removal with increasing metal concentration is due to the reduction in available active surface area at higher noble metal loading.

Table 2 summarizes a comparison of evaluated Pd (II) metal uptake from synthetic electroless plating with the data available in the literature for aqueous solutions. It can be observed that the evaluated metal uptake values are comparable with those evaluated for aqueous solutions with activated charcoal. Only for chitosan-modified adsorbents, higher metal uptake has been obtained and this is due to the enhanced adsorption characteristics of chitosan-modified resins. These resins cannot be compared with the activated charcoal adsorbents, given that the cost of activated charcoal is significantly lower than the cost of these resins. Among the available data, the data presented by Sharififard et al. [6] provides the best data in terms of maximum metal uptake. For aqueous solutions, the authors indicated that the adsorption capacities varied from 5.3 to 35.57 mg/g for a variation in palladium solution concentrations from 50 to 300 mg/L. In comparison with the data available in the literature for the adsorption of Pd(II) from aqueous solutions using AC, it can be observed that the capacities obtained in this work indicate lower metal uptake (32.41 mg/g) at higher Pd solution concentration (300 mg/L). Thus, it is apparent that the adsorption characteristics of synthetic electroless plating solutions are significantly different from those obtained with the aqueous solutions and this is due to the complex chemistry involved

Table 2
Comparison of the adsorbent capacity of the Pd(II) with activated carbon

Adsorbent	Solution	Pd solution concentration (mg/L)	Adsorbent capacity (mg/g)	Refs.
Activated carbon	Aqueous	50–300	5.3–35.7	[6]
BPMC	Aqueous	50–300	6–43.4	[6]
Activated carbon	Aqueous chloride solution	20–225	1.5–27	[7]
Cross-linked chitosan resin	Aqueous	50–400	9.5–109.7	[8]
Racomitrium lanuginosum	Aqueous	25–300	5–30.2	[10]
BTICF	Aqueous	43.8–48.8	22.4–27.5	[11]
Thiourea-modified chitosan	Aqueous	10–400	8.28–112.4	[12]
Activated carbon	Synthetic ELP solution	50–500	5.76–43.33 (agitation-assisted adsorption)	This work
Activated carbon	Synthetic ELP solution	50–500	6.34–45.5 (sonication)	This work
Activated carbon	Synthetic ELP solution + CTAB	50–500	6.69–50.13 (agitation-assisted adsorption)	This work
Activated carbon	Synthetic ELP solution + CTAB	50–500	7.52–60.03 (sonication)	This work

with other additives such as Na_2EDTA and liquor ammonia.

3.2.2.2. Pd(II) adsorption from electroless plating solutions containing CTAB surfactant. Fig. 5(b) summarizes the variation of adsorption capacities and removal for Pd (II) adsorption on AC in the presence of CTAB at its solution concentration of 2 CMC. As shown, the surfactant presence in the solution significantly influenced the Pd(II) adsorption characteristics on AC. A typical adsorption characteristic of heavy and noble metals from aqueous solutions refers to an increase in capacity and reduction in removal efficiency with increasing metal solution concentration. While this trend is seen even in the presence of CTAB surfactant, there is a significant increase in the adsorption parameters when compared to the ELP solutions without surfactant. The significant increase in metal uptake is attributed to the presence of the surfactant which alters the pertinent interfacial and surface characteristics of the adsorbent.

As shown in Fig. 5(b)—(i), for the agitation-assisted adsorption case, the capacities and % adsorption varied from 6.69–50.13 mg/g and 80.32–60.16% with variation in Pd solution concentration from 50 to 500 mg/L. On the other hand, for the case of sonication-assisted adsorption (Fig. 5(b)—(ii)), the capacities and % adsorption varied from 7.52–60.03 mg/g and 90.32–72.03% for a variation in Pd solution concentration from 50 to 500 mg/L. Therefore, once again, it can be inferred that sonication did not significantly enhance the capacity and removal percentage when compared to the agitation-assisted adsorption. The increase in metal uptake and adsorption efficiency values can again be attributed to the enhancement of adsorbent characteristics due to presence of the surfactant. In the literature, only one article addressed the removal of Cd(II) from aqueous solution using activated carbon impregnated with anionic surfactants [33] and no literature is available for the adsorption of surfactant containing Pd(II) solutions.

Table 2 summarizes the comparative variation of Pd(II) adsorption metal uptake from synthetic ELP solutions containing surfactant. In this work, the metal uptake for a Pd solution concentration of 300 mg/L corresponds to 34 mg/g, which is comparable lower (35.57 mg/g) with that reported by Sharififard et al. [6] for aqueous solutions. Also, the removal efficiency in this work is significantly lower (80.32%) than that reported by the authors (98%). Thus, the generalization of relating experimental adsorption data obtained for Pd(II) aqueous solution towards the design and operation of an adsorption process for electroless plating solution is not applicable, as significant variations exist for the removal efficiency.

3.2.2.3. Effect of surfactant solution concentration. Fig. 5(c)—(i) and (ii) respectively presents the variation of metal uptake and removal efficiency for the agitation-assisted adsorption of Pd(II) on activated charcoal for various cases of surfactant solution concentration (1–4 CMC). As shown, the metal uptake capacity increased with increasing surfactant solution concentration, which indicates that the insitu adsorption of surfactant on AC significantly favoured Pd adsorption as it leads to the improvement in the surface properties of the adsorbent. For a variation in Pd solution concentration from 50 to 500 mg/L, the metal uptake and removal efficiency varied from 6.31–6.8 mg/g and 75.78–56.16%, respectively, (1 CMC), which increased to 6.69–50.13 mg/g and 80.32–60.16%, respectively, at 2 CMC surfactant concentration and 7.19–51.83 mg/g and 86.32–62.19%, respectively, at 4 CMC surfactant concentration. Similar adsorption characteristics have been observed for the sonicated-assisted adsorption (Fig. 5(c)—(iii) and (iv)), where the metal uptake and efficiency respectively varied from 7.36–59.75 mg/g and 88.3–71.70% for 1 CMC surfactant concentration, 7.52–60.03 mg/g and 90.32–72.03% for 2 CMC surfactant concentration and 7.81–62.46 mg/g and 93.82–74.96% for 4 CMC surfactant concentrations. Once again it can be analysed that sonication performed marginally better than agitation-assisted adsorption of Pd(II). Thus, it is clearly evident that increasing surfactant solution concentration increased Pd adsorption in comparison with the case where surfactant was not involved. This is attributed to the role of surfactant adsorption on activated charcoal adsorbent. It is hypothesized that the surfactant strongly adsorbs to the commercial AC and thereby favours better binding of Pd groups to the chemically modified adsorbent. The observed trends are in agreement with the regime II and III of hypothesis presented by Paria and Khilar [34] and Fredrik et al. [35] for the surfactant adsorption on silica–water interface. The authors indicated that the surfactant adsorption can be presented in terms of a graph between the logarithmic plot of amount adsorbed and equilibrium concentration, which follows three distinct regimes [34,35]:

1. Regime I: this occurs at lower solution concentration and follows Henry's law to indicate a straight line profile with a slope of 1 for the adsorption characteristics.
2. Regime II: this occurs at higher solution concentration which provides higher adsorption capacity due to the interaction between the surfactants to result in their surface aggregation. The slope of the graph will be greater than 1 in this case.
3. Regime III: this indicates a slower rate of surfactant adsorption due to saturation and therefore the graph will have a slope lower than obtained for the Regime II.

However, it shall be noted that the literatures [34,35] elaborated upon surfactant adsorption during variation in surfactant solution concentrations but not upon heavy or noble metal adsorption in the presence of surfactant. Therefore, the direct relevance of hypothesis is an important issue that needs to be addressed in the near future.

3.3. Equilibrium and kinetic modelling

3.3.1. Adsorption equilibrium

Table 3 illustrates the fitness of Langmuir and Freundlich isotherm for both agitation-assisted adsorption and sonication-assisted Pd(II) adsorption on activated charcoal using synthetic electroless plating solutions not containing the cationic surfactant. For this case, it can be observed that both Langmuir and Freundlich isotherm models provide good fitness to represent the equilibrium adsorption data and among these two, Freundlich isotherm provided maximum fitness ($R^2 = 0.997$ and 0.987 for agitation-assisted adsorption and sonication-assisted adsorption, respectively). Thus, it is apparent that heterogeneous adsorption is the underlying physical mechanism. Corresponding summary of the RMS error values has been presented in Table 3, which indicates that Freundlich isotherm provided lowest error values. For the experimental data, the Freundlich isotherm modelling constants refer to $K_F = 0.768$ and $n = 1.34$ for agitation-assisted adsorption and $K_F = 1.21$ and $n = 1.45$ for sonication-assisted adsorption.

Table 4 and Fig. 6(a) and (b) summarize the results obtained for the fitness of Freundlich isotherm for the Pd(II) adsorption using synthetic electroless plating solutions containing CTAB surfactant. For this case as well, it has been evaluated that the Langmuir isotherm did not fit well with the measured experimental adsorption parameters ($R^2 = 0.835$ and 0.865 for agitation-assisted adsorption and sonication-assisted adsorption, respectively). On the other hand, the coefficient of correlation for the Freundlich equilibrium isotherm indicated better fitness ($R^2 = 0.993$ and 0.985 for agitation-assisted adsorption and sonication-assisted adsorption, respectively). The fitness plots presented in Fig. 6(a) and (b) for both Agitation and sonication-assisted adsorption respectively infers that Freundlich isotherm fits well for Pd solution concentrations within the range of 50–400 mg/L. At 500 mg/L, significant deviation was observed for the fitness.

Table 3
Langmuir and Freundlich isotherm fitness and model parameters for Pd(II) adsorption from synthetic electroless plating solutions without CTAB surfactant

			% Error					
Mass transfer technique	Model	R^2	RMS	Avg	Max	Min	Monolayer adsorption capacity, $q_{\max}$ (mg/g)	Model parameters
Agitation-assisted without CTAB	Langmuir	0.988	3.46	2.49	7.08	0.08	42.9	$b = 0.004$, $K_R = 0.703$
	Freundlich	0.997	1.56	1.02	1.66	0.004	–	$K_F = 0.768$, $n = 1.34$
Sonication without CTAB	Langmuir	0.989	4.56	3.52	7.65	0.40	52.4	$b = 0.007$, $K_R = 0.633$
	Freundlich	0.987	2.49	2.24	3.37	0.42	–	$K_F = 1.21$, $n = 1.45$

Table 4
Freundlich isotherm model fitness and model parameters for Pd(II) adsorption from CTAB surfactant consisting synthetic electroless plating solutions

			% Error				Model values	
Method	Surfactant concentration (CMC)	R^2	RMS	Avg	Max	Min	K_F	n
Sonication with CTAB	1	0.988	11.43	8.61	23.3	1.8	24.7	1.53
	2	0.986	10.88	8.85	19.7	1.28	28.8	3.23
	3	0.985	11.10	10.71	15.5	5.69	27.1	1.74
	4	0.993	7.24	6.60	10.3	0.46	33.4	1.47
Physisorption with CTAB	1	0.835	44.46	39.94	63.5	7.23	32.1	1.56
	2	0.963	18.23	16.37	26.89	2.65	23.7	3.65
	3	0.978	14.28	11.19	29.66	3.98	23.3	2.45
	4	0.985	11.06	9.78	17	0.6	23.1	1.71

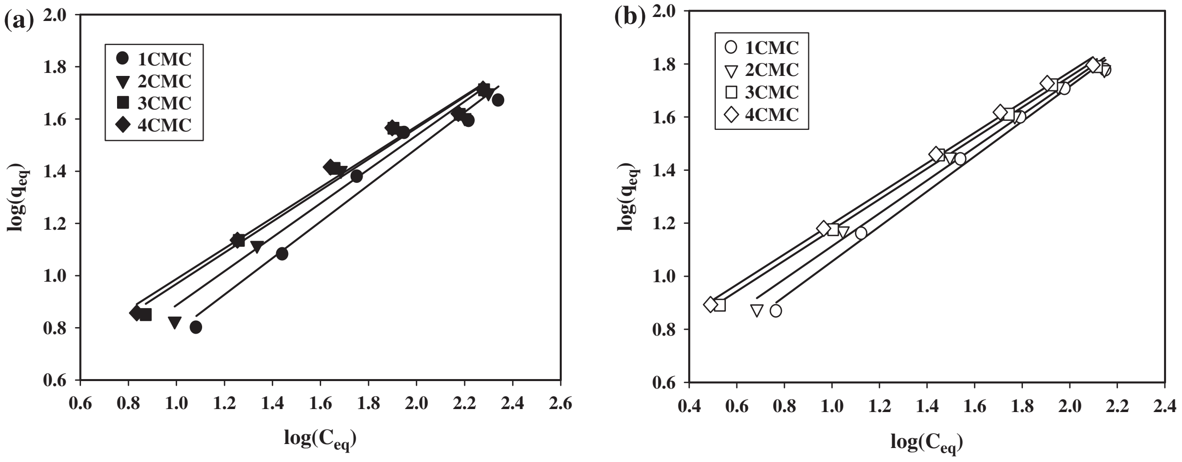

Fig. 6. Freundlich isotherm fitness plots for Pd(II) adsorption of Pd(II) from synthetic electroless plating solutions containing CTAB surfactant (1–4 CMC)—(a) agitation and (b) sonication-assisted adsorption.

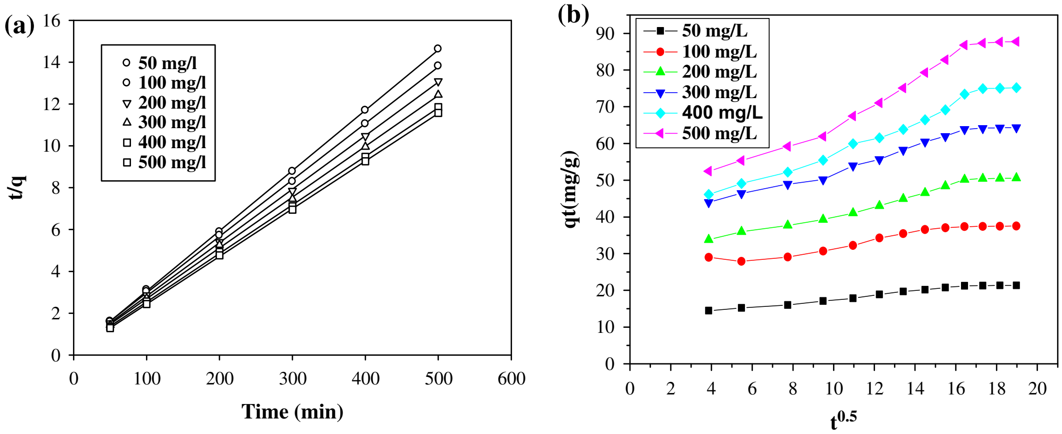

Fig. 7. Fitness plots for Pd(II) adsorption from synthetic electroless plating solutions with 2 CMC surfactant concentration —(a) pseudo-second-order kinetic model and (b) intra-particle diffusion model.

Table 5

Pseudo-second-order kinetic model parameters for Pd(II) removal from synthetic electroless plating solutions (a) without surfactant and (b) with 2 CMC CTAB surfactant concentration

	q_e (mg/g)				% Error			
C_e (mg/L)	Exp	Cal	R^2	$k_2 \times 10^{-3}$ (L/min)	RMS	Avg	Max	Min
50	21.75	22.37	0.99	4.7	0.99	0.66	2.18	0.008
100	36.36	37.03	0.99	2.6	1.36	1.09	2.43	0.21
200	38.50	39.06	0.99	2.5	0.93	0.80	1.36	0.23
300	41.21	41.15	0.99	2.2	1.90	1.36	3.65	0.15
400	42.75	43.19	0.99	2.2	1.57	1.04	3.49	0.01
500	43.28	44.32	0.99	2.4	4.13	3.66	7.58	2.07

3.3.2. Adsorption kinetics

Among the two kinetic models tested for their fitness towards representing experimentally measured kinetic data of Pd(II) adsorption on activated charcoal in the presence of CTAB surfactant, it has been evaluated that the first-order model did not fit well as the plots did not pass through the origin. However, good fitness was observed for the second-order kinetic model. Fig. 7(a) presents the fitness of the second-order kinetic model for the measured kinetic data for the case of 2 CMC surfactant solution concentration and Pd solution concentrations varying from 50 to 500 mg/L. Corresponding model parameters and errors are summarized in Table 5. As presented in Table 5, there is a good agreement with the q_e values determined experimentally and from pseudo-second-order model. Similar modelling trends were observed for other sets of surfactant concentrations but are not shown. The kinetic results were further analysed with intra-particle diffusion model to elaborate upon the pertinent diffusion mechanism of Pd(II) adsorption with ELP solutions consisting of 2 CMC surfactant. The fitness of measured Pd(II) adsorption kinetic data towards the intra-particle diffusion model is presented in Fig. 7(b) which affirms upon the existence of two distinct adsorption characteristics. These correspond to initial sharper region where instantaneous external surface adsorption occurs on the adsorbent and the later gradual Pd adsorption that involves intra-particle diffusion as a rate limiting step. At longer time periods, it can be observed that saturation is apparent. These observations are in agreement with the literature [6].

3.4. Thermodynamic parameters

Since only Pd(II) adsorption data obtained using synthetic electroless plating solutions without CTAB surfactant follow Langmuir equilibrium model, thermodynamic model parameters have been evaluated for this case only and correspond to 37.8 kJ/mol and 1.94 kJ/K. mol, respectively, for agitation-assisted adsorption and 49.3 kJ/mol and 1.8 kJ/K. mol for sonication, respectively. The obtained thermodynamic parameter values are positive and thereby indicate the Pd(II) adsorption from synthetic electroless plating solutions is spontaneous and endothermic nature [36].

3.5. Desorption characteristics

For the Pd-AC adsorbent prepared with 300 mg/L initial solution concentration, the experimentally evaluated metal capacity is 36.53 mg/g. Using 0.1 M HCl, the equilibrium Pd concentration on the adsorbent after adsorption was evaluated to be 80.85 mg/L. Using these two values, the batch desorption efficiency is about 2.25% which is significantly low. Similarly using 0.1 M NaOH, the adsorbent Pd concentration and batch desorption efficiency were evaluated as 39.7 mg/L and 4.45%. Thus, comparing these two cases, it can be concluded that strong irreversible chemisorption occurred during Pd(II) adsorption on AC, as the elution efficiency has been significantly low. Among HCl and NaOH, NaOH provided better elution characteristics as the PZC of AC is in the basic media range.

4. Conclusions

This work presented Pd(II) adsorption characteristics on activated charcoal from synthetic Pd electroless plating solutions without and with CTAB cationic surfactant. Optimal operating conditions for batch adsorption were identified as contact time = 300 min, pH 10, dosage 6 g/L within the concentration range of 50–500 mg/L Pd solution concentration. It was observed that the Pd(II) adsorption characteristics from synthetic electroless plating solutions are significantly different from Pd(II) adsorption from aqueous solutions. While the ELP solutions containing the surfactant indicated the expected trend of increasing metal uptake and decreasing adsorption efficiency with increasing concentration, the adsorption process variable values obtained were significantly higher than what were obtained for the corresponding concentrations in the case of ELP solutions without the surfactant. The surfactant containing solutions provided enhancement in metal uptake with increasing concentration. The metal uptake values varied from 5.76 to 43.33 mg/g and the values for removal efficiency varied from 69.12 to 52% with increasing Pd solution concentration. For ELP solutions with surfactants, the values of metal uptake varied from 6.69 to 50.13 mg/g and removal efficiency varied from 80.32 to 60.16%.

Also, the evaluated adsorption characteristics are distinct and indicate higher metal uptake and removal efficiency than those obtained for aqueous solutions. It has been observed that sonication-assisted adsorption performed marginally better than the agitation-assisted adsorption case for metal uptake and removal efficiency values. Also, for a given solution Pd(II) concentration, it has been observed that both metal uptake and removal efficiency values increased with increasing CTAB surfactant solution concentration, thus indicating that surfactant significantly altered the prevalent surface phenomena associated to Pd adsorption on AC. For all cases, Freundlich equilibrium isotherm and pseudo-second-order kinetic model have been evaluated to be the best fit models. In summary, while similar metal uptakes were obtained, lower removal efficiencies were obtained for the case of synthetic ELP solutions in comparison with aqueous solutions. Thus, the experimental and theoretical adsorption characteristics of Pd(II) are anticipated to serve as reference data for the cost-effective recovery and reuse of Pd(II) from spent electroless plating solutions using activated charcoal adsorbent. Future work needs to affirm upon the development of suitable models to primarily analyse the functionality of surfactant during Pd(II) adsorption on activated carbon.

References

[1] Occupational Safety and Health Administration (OSHA), Permissible exposure limit (PEL) for various elements and compounds. Available from: <http://www.osha.gov/dsg/topics/pel/>.

[2] J. Kielhorn, C. Melber, D. Keller, I. Mangelsdorf, Palladium—A review of exposure and effects to human health, Int. J. Hyg. Environ. Health 205 (2002) 417–432.

[3] A. Dakshinamoorthy, P.S. Dhami, P.W. Naik, N.L. Dudwadkar, S.K. Munshi, P.K. Dey, V. Venugopal, Separation of palladium from high level liquid waste of PUREX origin by solvent extraction and precipitation methods using oximes, Desalination 232 (2008) 26–36.

[4] Y. Xu, Z. Chen, J. Yan, S. Dong, Method for recovery of gold and palladium from spent electroplating liquor, Faming Zhuanli Shenqing Gongkai shuomingshu. CN 85100240 A (1986) 7–16.

[5] N. Warner, M.L. Free, J. Miner, The electrochemical recovery of metallic palladium from spent electroless plating solution, JOM 61(10) (2009) 27–30.

[6] H. Sharififard, M. Soleimani, F.Z. Ashtiani, Evaluation of activated carbon and bio-polymer modified activated carbon performance for palladium and platinum removal, J. Taiwan Inst. Chem. Eng. 43 (2012) 696–703.

[7] H. Kasaini, M. Goto, S. Furusaki, Selective separation of Pd(II), Rh(III), and Ru(III) ions from a mixed chloride solution using activated carbon pellets, Sep. Sci. Technol. 35 (2000) 1307–1327.

[8] K. Fujiwara, A. Ramesh, T. Maki, H. Hasegawa, K. Ueda, Adsorption of platinum(IV), palladium(II) and gold(III) from aqueous solutions onto l-lysine modified crosslinked chitosan resin, J. Hazard. Mater. 146 (2007) 39–50.

[9] S. Morisada, Y.H. Kim, T. Ogata, Y. Marutani, Y. Nakano, Improved adsorption behaviors of amine-modified tannin gel for palladium and platinum ions in acidic chloride solutions, Ind. Eng. Chem. Res. 50 (2011) 1875–1880.

[10] A. Sari, D. Mendil, M. Tuzen, M. Soylak, Biosorption of palladium(II) from aqueous solution by moss (*Racomitrium lanuginosum*) biomass: Equilibrium, kinetic and thermodynamic studies, J. Hazard. Mater. 162 (2009) 874–879.

[11] H.W. Ma, X.P. Liao, X. Liu, B. Shi, Recovery of platinum(IV) and palladium(II) by bayberry tannin immobilized collagen fiber membrane from water solution, J. Membr. Sci. 278 (2006) 373–380.

[12] H.U. Foersterling, M. Beer, K.H. Hallmeier, Investigations of the adsorption of palladium on carbonaceous adsorbents modified with dimethylglyoxime, II the adsorption of palladium on a lignite in its unmodified form and modified with dimethylglyoxime, Carbon 28 (4) (1990) 503–508.

[13] D. Parajuli, H. Kawakita, K. Inoue, M. Funaoka, Recovery of gold(III), palladium(II), and platinum(IV) by aminated lignin derivatives, Ind. Eng. Chem. Res. 45 (2006) 6405–6412.

[14] O. Kononova, A.G. Kholmogorov, N.V. Danilenko, N.G. Goryaeva, K.A. Shatnykh, S.V. Kachin, Recovery of silver from thiosulfate and thiocyanate leach solutions by adsorption on anion exchange resins and activated carbon, Hydrometallurgy 88 (2007) 189–195.

[15] L. Zhou, J. Liu, Z. Liu, Adsorption of platinum(IV) and palladium(II) from aqueous solution by thiourea-modified chitosan microspheres, J. Hazard. Mater. 172 (2009) 439–446.

[16] C.I. Park, J.S. Chung, K.W. Cha, Separation and pre concentration method for palladium, platinum and gold from some heavy metals using amberlite IRC 718 chelating resin, Korean Chem. Soc. 21(1) (2000) 121–124.

[17] Y. Rajesh, M. Pujari, R. Uppaluri, Equilibrium and kinetic studies of Ni(II) adsorption using pineapple and bamboo stem based adsorbents, Sep. Sci. Technol. 49(4) (2014) 533–544.

[18] P.V. Sunder Raju, Comparison of different extraction methods to determine gold in geological samples, J. Sci. Ind. Res. 65 (2006) 65–67.

[19] Y.S. Ho, C.T. Huang, H.W. Huang, Equilibrium sorption isotherm for metal ions on tree fern, Process Biochem. 37 (2002) 1421–1430.

[20] I. Langmuir, The adsorption gases on plane surface of glass, mica and platinum, J.A.C.S. 40 (1916) 1316–1368.

[21] M.F. Freundlich, Over the adsorption in solution, J. Phys. Chem. B 57 (1906) 385–470.

[22] C. Aharoni, M. Ungarish, Kinetics of activated chemisorption, Part 2, theoretical model, J. Chem. Soc. 73 (1977) 456–464.

[23] Y.S. Ho, G. McKay, Pseudo-second order model for sorption processes, Process Biochem. 34 (1999) 451–465.

[24] Y.S. Ho, Review of second order models for adsorption systems, J. Hazard. Mater. 136 (2006) 681–689.

[25] V.C. Srivastava, M.M. Swamy, I.D. Mall, B. Prasad, I.M. Mishra, Adsorptive removal of phenol by bagasse fly ash and activated carbon: Equilibrium, kinetics and thermodynamics, Colloids Surf., A 272 (2006) 89–104.

[26] S. Brunauer, P.H. Emmett, E. Teller, Adsorption of gases in multimolecular layers, J. Am. Chem. Soc. 60 (1938) 309–319.

[27] K.S.W. Sing, D.H. Everett, R.A.W. Haul, L. Moscou, R.A. Pierotti, J. Rouquerol, T. Siemieniewska, Reporting physisorption data for gas and solid systems with special reference to the determination of surface area and porosity, Pure Appl. Chem. 57 (1985) 603–619.

[28] L.D. Gelb, K.E. Gubbins, Pore size distributions in porous glasses: A computer simulation study, Langmuir 15 (1999) 305–308.

[29] S.A. Dastgheib, D.A. Rockstraw, A model for the adsorption of single metal ion solutes in aqueous solution onto activated carbon produced from pecan shells, Carbon 40 (2002) 843–851.

[30] X. Ma, F. Ouyang, Adsorption properties of biomass-based activated carbon prepared with spent coffee grounds and pomelo skin by phosphoric acid activation, Appl. Surf. Sci. 268 (2013) 566–570.

[31] C.A. Snyders, C.N. Mpinga, S.M. Bradshaw, G. Akdogan, J.J. Eksteen, The application of activated charcoal from the adsorption and elution of platinum group metals from dilute cyanide leach solutions, J. South. Inst. Min. Metall. 113 (2013) 381–388.

[32] Y. Yang, Y. Chun, G. Sheng, M. Huang, pH-dependence of pesticide adsorption by wheat-residue-derived black carbon, Langmuir 20 (2004) 6736–6741.

[33] C.K. Ahn, D. Park, S.H. Woo, J.M. Park, Removal of cationic heavy metal from aqueous solution by activated carbon impregnated with anionic surfactants, J. Hazard. Mater. 164(2–3) (2009) 1130–1136.

[34] S. Paria, K.C. Khilar, A review on experimental studies of surfactant adsorption at the hydrophilic solid–water interface, Adv. Colloid Interface Sci. 110 (2004) 75–95.

[35] T. Fredrik, B. Jonson, B. Lindeman, Ellipsometry studies of the self-assembly of non-ionic surfactants at the silica-water interface: Kinetic aspects, Langmuir 10 (1994) 3714–3722.

[36] L. Jossens, J.M. Prausnitz, W. Fritz, E.U. Schlünder, A.L. Myers, Thermodynamics of multi-solute adsorption from dilute aqueous solutions, Chem. Eng. Sci. 33 (1978) 1097–1106.